Development 133, 2325-2335 (2006) doi:10.1242/dev.02394

Gli3-mediated somitic *Fgf10* expression gradients are required for the induction and patterning of mammary epithelium along the embryonic axes

Jacqueline M. Veltmaat[1,2,*], Frédéric Relaix[3], Lendy T. Le[1], Klaus Kratochwil[1], Frédéric G. Sala[1,2], Wendy van Veelen[2,†], Ritva Rice[4], Bradley Spencer-Dene[5], Arnaud A. Mailleux[2,‡], David P. Rice[4], Jean Paul Thiery[2] and Saverio Bellusci[1,2]

Little is known about the regulation of cell fate decisions that lead to the formation of five pairs of mammary placodes in the surface ectoderm of the mouse embryo. We have previously shown that fibroblast growth factor 10 (FGF10) is required for the formation of mammary placodes 1, 2, 3 and 5. Here, we have found that *Fgf10* is expressed only in the somites underlying placodes 2 and 3, in gradients across and within these somites. To test whether somitic FGF10 is required for the formation of these two placodes, we analyzed a number of mutants with different perturbations of somitic *Fgf10* gradients for the presence of WNT signals and ectodermal multilayering, markers for mammary line and placode formation. The mammary line is displaced dorsally, and formation of placode 3 is impaired in $Pax3^{lLZ/lLZ}$ mutants, which do not form ventral somitic buds. Mammary line formation is impaired and placode 3 is absent in $Gli3^{Xt\text{-}J/Xt\text{-}J}$ and hypomorphic *Fgf10* mutants, in which the somitic *Fgf10* gradient is shortened dorsally and less overall *Fgf10* is expressed, respectively. Recombinant FGF10 rescued mammogenesis in $Fgf10^{-/-}$ and $Gli3^{Xt\text{-}J/Xt\text{-}J}$ flanks. We correlate increasing levels of somitic FGF10 with progressive maturation of the surface ectoderm, and show that full expression of somitic *Fgf10,* co-regulated by GLI3, is required for the anteroposterior pattern in which the flank ectoderm acquires a mammary epithelial identity. We propose that the intra-somitic *Fgf10* gradient, together with ventral elongation of the somites, determines the correct dorsoventral position of mammary epithelium along the flank.

KEY WORDS: Ectodermal patterning, Mammary gland, Somites, Placode individuality, FGF10/FGFR2B, GLI3, PAX3, WNT signaling, Mouse

INTRODUCTION

Mammogenesis in the mouse starts around embryonic day 10.5 (E10.5) with the formation of three separate streaks on both flanks. These streaks consist of multilayered surface ectoderm, specifically expressing *Wnt10b* (Veltmaat et al., 2004) and engaged in canonical WNT signaling (Chu et al., 2004). The first streak forms the mammary line between the forelimb and hindlimb, and mammary placode 3 develops first on this line at E11.0-E11.5 (Mailleux et al., 2002; Eblaghie et al., 2004; Veltmaat et al., 2004). Meanwhile, the inguinal and axillary streaks arise, from which placodes 5 and 1, respectively, form. Placodes 4 and 2 emerge where the mammary line abuts these respective streaks (Veltmaat et al., 2004).

Few genes are known to be involved in early mammogenesis (Mustonen et al., 2003; Chu et al., 2004; Mustonen et al., 2004; Howard et al., 2005; Jerome-Majewska et al., 2005). Most of them are expressed in the ectoderm, yet factors from the underlying mesenchyme initiate mammogenesis (Veltmaat et al., 2003). We have previously shown that FGF10 signaling via the FGF receptor isoform 2b (FGFR2B) is required for the formation of mammary placodes 1, 2, 3 and 5. We proposed the ventral (hypaxial) dermomyotome of the somites as the source of FGF10 (Mailleux et al., 2002). Hypaxial FGF10 may be a mesenchymal initiator of mammogenesis, as it could reach the ectodermal FGFR2B either via diffusion through the thin lateral plate mesoderm or via delamination of hypaxial cells.

The emergence of the mammary line as fragments overlying the hypaxial somitic buds further suggested an involvement of hypaxial somitic signals in induction (Veltmaat et al., 2004). However, only the thoracic somites 11-24 between the forelimb and hindlimb possess hypaxial buds (Eloy-Trinquet, 2000). Therefore, we now hypothesize that hypaxial signals are important only for the formation of the mammary line on which mammary placodes 2, 3 and 4 form (Fig. 1), whereas other sources of signals may be decisive for the formation of the streaks on which placodes 1 and 5 form. As placode 4 forms in the absence of FGF10/FGFR2B signaling, the requirement for hypaxial FGF10 would thus be restricted to the formation of placodes 2 and 3 only.

To test this hypothesis, we examined mammary development in *Pax3* null mutants that lack the hypaxial somitic buds (Relaix et al., 2003); in *Gli3* null and *Fgf10* hypomorphic embryos, both expressing reduced levels of somitic *Fgf10*; in *Fgf10* and *Fgfr2b* null embryos; and by applying recombinant FGF10. We identified a signaling cascade involving somitic GLI3 upstream of FGF10 within the somites, which in turn activates ectodermal FGFR2B, leading to *Wnt10b* expression and canonical WNT signaling. This cascade is required for the induction and correct positioning of the

[1]The Saban Research Institute of Childrens Hospital Los Angeles/University of Southern California, Developmental Biology Program, Los Angeles, CA 90027, USA. [2]Institut Curie/CNRS-UMR144, Equipe de Morphogenèse Cellulaire et Progression Tumorale, 75005 Paris, France. [3]Institut Pasteur/CNRS-URA 2578, Département de Biologie Moléculaire, Génétique Moléculaire du Développement, 75015 Paris, France. [4]King's College, Departments of Orthodontics and Craniofacial Development, London SE1 9RT, UK. [5]Cancer Research UK, London Research Institute, Experimental Pathology Laboratory, and Imperial College London, Department of Histopathology, London WC2A 3PX, UK.

[†]Present address: Universitair Medisch Centrum Utrecht, Afdeling Metabole en Endocriene Ziekten, Divisie Biomedische Genetica, 3584 EA Utrecht, The Netherlands

[‡]Present address: Harvard Medical School, Department of Cell Biology, Boston, MA 02115, USA

*Author for correspondence (e-mail: jveltmaat@chla.usc.edu and jmveltmaat@hotmail.com)

Accepted 4 April 2006

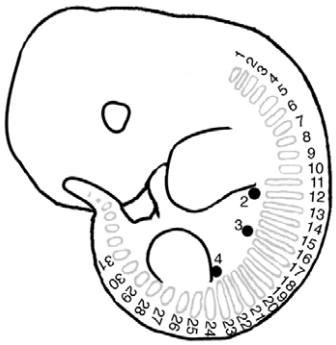

Fig. 1. The position of mammary rudiments relative to the somites. E11 embryo with the somites (numbered) indicated as grey contours. Only the thoracic somites 11-24 possess a ventrally elongated hypaxial bud, underlying the region where mammary placodes 2, 3 and 4 develop (black dots). Mammary placodes 1 and 5 are covered by the forelimb and hindlimb, respectively, and are not indicated.

mammary line on the flank, and indispensable for the formation of placode 3. We propose that correct patterning is achieved through a combination of somitic elongation and somitic *Fgf10* gradients.

MATERIALS AND METHODS

Mice

Fgf10$^{+/-}$ (Sekine et al., 1999) and *Gli3*$^{Xt\text{-}J/+}$ mice [Jackson Laboratories, stock 00026; for genotyping see Maynard et al. (Maynard et al., 2002)] were maintained on a C57BL/6 background; *Fgfr2b*$^{+/-}$ mice (De Moerlooze et al., 2000) were maintained on a mixed C57BL/6×GK129 background; TOPGAL mice (DasGupta and Fuchs, 1999) were maintained on a CD1 background and backcrossed at least three generations with the mutants above on their respective backgrounds; *Pax3*$^{ILZ/+}$ mice (Relaix et al., 2003) were maintained on a mixed C57BL/6×BCA background; and *Fgf10*$^{Mlc1v\text{-}nLacZ\text{-}v24}$ (here *Fgf10*^{mlcv}) mice (Kelly et al., 2001) were maintained on a mixed agouti background. The latter were mated with *Fgf10*$^{+/-}$ mice to obtain *Fgf10*$^{mlcv/-}$ hypomorphic embryos. Noon of the day of a vaginal plug was considered E0.5. Mutant embryos were stage matched with their littermate controls on the basis of somite counts.

X-gal staining

Pax3$^{ILZ/ILZ}$, TOPGAL and *Fgf10*^{mlcv} embryos were fixed in 4% PFA/D-PBS and stained with 1 mg X-gal/ml dimethylformamide in 5 mM $K_3Fe(CN)_6$/5 mM $K_4Fe(CN)_6$/2 mM $MgCl_2$ in D-PBS pH 7.4 to reveal β-galactosidase (*lacZ*) activity.

RNA in situ hybridization

Whole-mount in situ hybridization was performed as described (Veltmaat et al., 2004) with digoxigenin-labeled riboprobes of *Fgf10* (Bellusci et al., 1997), *Wnt10b* or *Lef1*. Paraffin sections (10 μm) were hybridized with [^{35}S]UTP labeled riboprobes of *Fgfr1b, Fgfr1c*, *Fgfr2b*, *Fgfr2c*, *Fgfr3b*, *Fgfr3c* (Kettunen et al., 1998) and *Fgfr4* (Partanen et al., 1991) and analyzed as described (Rice et al., 2000).

Explant culture and application of recombinant FGF10

Eviscerated embryonic flanks were cultured as described for tooth anlagen (Kratochwil et al., 2002). Heparin-acrylic beads (Sigma) were incubated in D-PBS containing 100 ng BSA/μl with or without 100 ng rFGF10 (R&D Systems)/μl, and implanted underneath the surface ectoderm, at the hypaxial bud of somite 14-15 or 17-18. After 2-3 days of culture, explants were processed for whole-mount in situ hybridization or X-gal staining.

Histology

Specimens fixed in 60% methanol/30% $CHCl_3$/10% HAc or 4% PFA/D-PBS were embedded in paraffin wax, sectioned (6 μm) and stained with Hematoxylin/Eosin or Nuclear Fast Red (Lab Vision Corporation), respectively.

RESULTS

The absence of hypaxial somitic buds correlates with impaired initiation of mammogenesis

To test whether hypaxial signals are required for the initiation of mammogenesis, we analyzed mammary line formation in *Pax3*$^{ILZ/ILZ}$-null mutant embryos. These mutants lack the hypaxial buds of somites 11-24, as shown by the shortened domain of somitic *lacZ* expression replacing *Pax3* expression (Fig. 2A-D) (Relaix et al., 2003). Somites 11-24 are located between the forelimb and hindlimb, underlying the mammary line and placodes 2, 3 and 4 (Fig. 1, Fig. 2A).

Whole-mount in situ hybridization shows that *Wnt10b* is expressed at reduced levels and in a narrower line on the flank of *Pax3*$^{ILZ/ILZ}$ embryos compared with control littermates (Fig. 2E-H). Placode 3 forms a day late, while the other placodes emerge in time (Fig. 2I,J, and not shown). Furthermore, *Wnt10b* expression is not attenuated between the placodes, and seems to be located slightly more dorsal in *Pax3*$^{ILZ/ILZ}$ mutants. Transverse sections demonstrate that the mammary line is located at the level of the notochord in *Pax3*$^{ILZ/ILZ}$ mutants, but more ventrally in control embryos (lines in Fig. 2K-N). The narrower width of the mammary line in *Pax3*$^{ILZ/ILZ}$ mutants, as inferred from *Wnt10b* expression (Fig. 2F), correlates with a narrower band of multilayered ectoderm (between asterisks in Fig. 2O,P), which moreover contains one cell layer less than in control embryos (Fig. 2O,P). This phenotype strongly suggests that hypaxial signals are required for the correct temporal formation and dorsoventral position of the mammary line and placode 3, but surprisingly, not for the formation of placodes 2 and 4, and as expected, not for placodes 1 and 5.

Our previous data had suggested that at E10.5, the hypaxial buds produce the FGF10 required for mammary placode formation (Mailleux et al., 2002). However, by E11.25 (43 somites), *Fgf10* expression extends throughout the entire thoracic somites 12-18 spanning the region underlying mammary placodes 2 and 3, while expression is highest in the hypaxial buds (Fig. 2Q). This domain of highest *Fgf10* expression is absent in the somites of *Pax3*$^{ILZ/ILZ}$ mutant embryos, while the level of *Fgf10* expression in the central part of the somites seems unaffected (Fig. 2R). As mammary placode 3 is formed in *Pax3*$^{ILZ/ILZ}$ mutants, and *Pax3* is neither expressed in the surface ectoderm nor in the underlying mesenchyme (Fig. 2A,C) (Relaix et al., 2003), we now hypothesize that both hypaxial and central somitic *Fgf10* are required for the formation of placode 3, and perhaps for the mammary line prior to placode formation.

Defective initiation in mammogenesis in *Fgf10*$^{-/-}$ and *Fgfr2b*$^{-/-}$ mutants

To test this hypothesis, we examined ectodermal maturation in detail and determined when the defect in mammogenesis becomes first apparent in *Fgf10*$^{-/-}$ and *Fgfr2b*$^{-/-}$ embryos. Normally, the surface ectoderm starts out as a single layer, the stratum germinativum, of squamous cells (Fig. 3A,B). At the Wolffian ridge (i.e. the flank), these cells become cuboidal and covered by a layer of squamous periderm by E8 (Fig. 3C) (Sengel, 1976; Stephens, 1982). By E11.5 (45 somites) the cells of the stratum germinativum become cylindrical at the flank while remaining squamous ventral and dorsal to the flank (Sengel, 1976) (Fig. 3B). Subsequently, one or two non-stratified layers of cylindrical cells form the stratum intermedium between the stratum germinativum and the periderm (Sengel, 1976). We show that this multilayering occurs first ventrally on the flank, and co-localizes with *Wnt10b* expression (Fig. 3D,G), indicative for the formation of the mammary line and the individual placodes. In

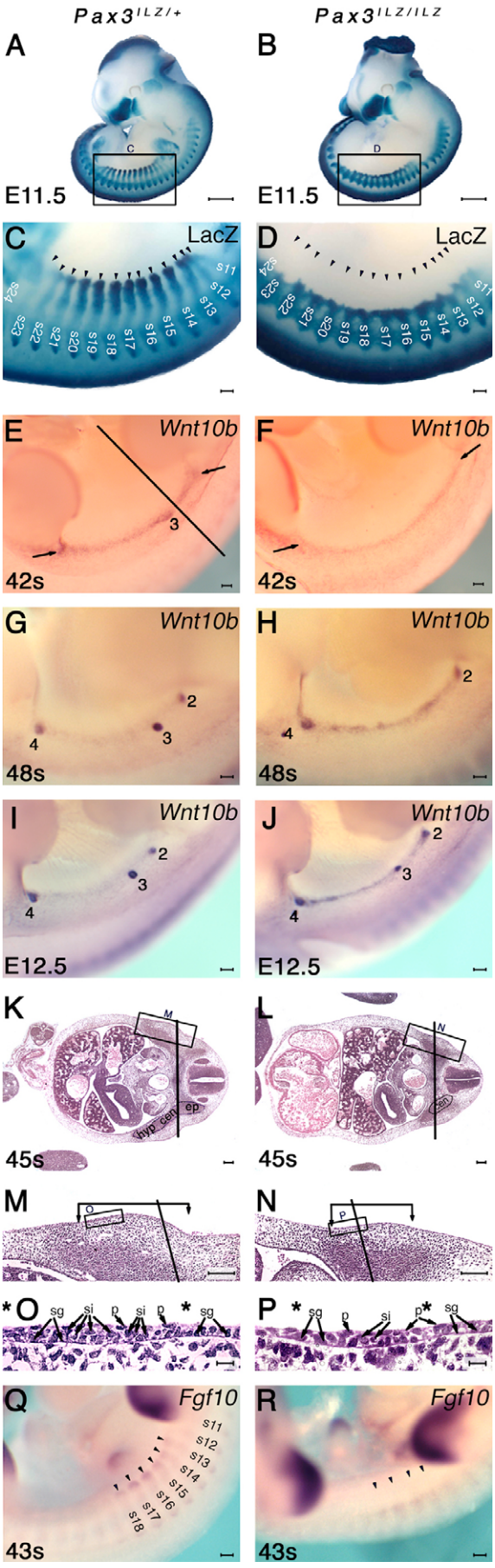

Fig. 2. The absence of hypaxial *Fgf10* expression correlates with a mammary phenotype in *Pax3*$^{ILZ/ILZ}$ embryos. (**A-D**) X-Gal staining revealing *Pax3-lacZ* expression; the boxed area in A and B is magnified in C and D. The hypaxial buds, indicated by black arrowheads, of the somites (numbered) are absent in the mutant. (**E-J**) Whole-mount in situ hybridization at E11.25 (42 somite), E11.75 (48 somite) and E12.5 for *Wnt10b*, revealing the mammary line (between the arrows in E,F) and placodes (numbered in G-J), demonstrates late formation of placode 3 in the mutant. (**K-P**) Hematoxylin-Eosin stained sections through the plane indicated by the black line in E. The vertical line in K-N through the notochord illustrates the more dorsal position of the mammary line in mutants. The horizontal line with downwards arrows (M,N) demarcates the area containing cylindrical ectodermal cells, while the area between the asterisks (O,P) contains a stratum intermedium as a hallmark of the mammary line. Both areas are narrower in mutants. (**Q-R**) Whole-mount in situ hybridization for *Fgf10* at E11.5. The hypaxial domain with high *Fgf10* expression (black arrowheads) is absent in the mutant (R). Abbreviations: s, somite stage; sg, stratum germinativum; si, stratum intermedium; p, periderm. Scale bars: 10 μm in O,P; 100 μm in C-J,M,N,Q,R; 1 mm in A,B,K,L.

E11.5-E11.75 (44-47 somites) *Fgf10*$^{-/-}$ and *Fgfr2b*$^{-/-}$ embryos, the cells of the stratum germinativum of the flank are cuboidal instead of cylindrical (Fig. 3E,F), and formation of the periderm is impaired. Furthermore, the stratum intermedium and *Wnt10b* expression are absent (Fig. 3E,F,H,I), except in the area of placode 4. There, a small streak of weak *Wnt10b* expression coincides with the formation of a stratum intermedium composed of cuboidal instead of cylindrical cells (not shown). As the role of WNT10B in mammary line formation is unknown, but canonical WNT signaling is required (Chu et al., 2004), we crossed *Fgf10*$^{+/-}$ and *Fgfr2b*$^{+/-}$ mice with mice carrying the TOPGAL transgenic reporter for canonical WNT signaling (DasGupta and Fuchs, 1999), used here as a functional marker for mammary line and placode formation (Fig. 3Q,R). Like *Wnt10b* expression, TOPGAL expression is weak, and restricted to the area of placode 4 in E11.5 (46 somites) *Fgf10*$^{-/-}$ and *Fgfr2b*$^{-/-}$ mutants (Fig. 3J-L). Accordingly, the expression pattern of *Lef1*, another early marker for mammogenesis (Mailleux et al., 2002) demonstrates that all buds except 4 are absent at E12.5 (Fig. 3M-O). We conclude that ectodermal maturation preceding mammary line formation requires FGF10/FGFR2B signaling, except in the region of placode 4. If FGFR2B is activated by somitic FGF10, then central somitic *Fgf10* expression appears sufficient for initiation, as seen in *Pax3*$^{ILZ/ILZ}$ mutants. Additional hypaxial *Fgf10* expression is required for the normal formation of the stratum intermedium, a hallmark of the mammary line, and for the correct temporal formation of placode 3.

Expression patterns support a role for hypaxial and central somitic Fgf10 in mammogenesis

To further determine the precise *Fgf10* expression domain responsible for the formation of the mammary line, we analyzed *Fgf10* expression from E7.5 onwards. Whole-mount in situ hybridization reveals *Fgf10* expression only in the head region until E9 (not shown). At E9.5-10 (26-30 somites), expression is also detected in the heart, the lateral plate mesoderm and limb bud mesenchyme (Fig. 4A,B). Around E10.25, *Fgf10* expression is further detectable in the hypaxial bud of thoracic somites 11-13 at the position of the prospective placode 2, whereas it is no longer detectable in the lateral plate mesenchyme of the flank (not shown).

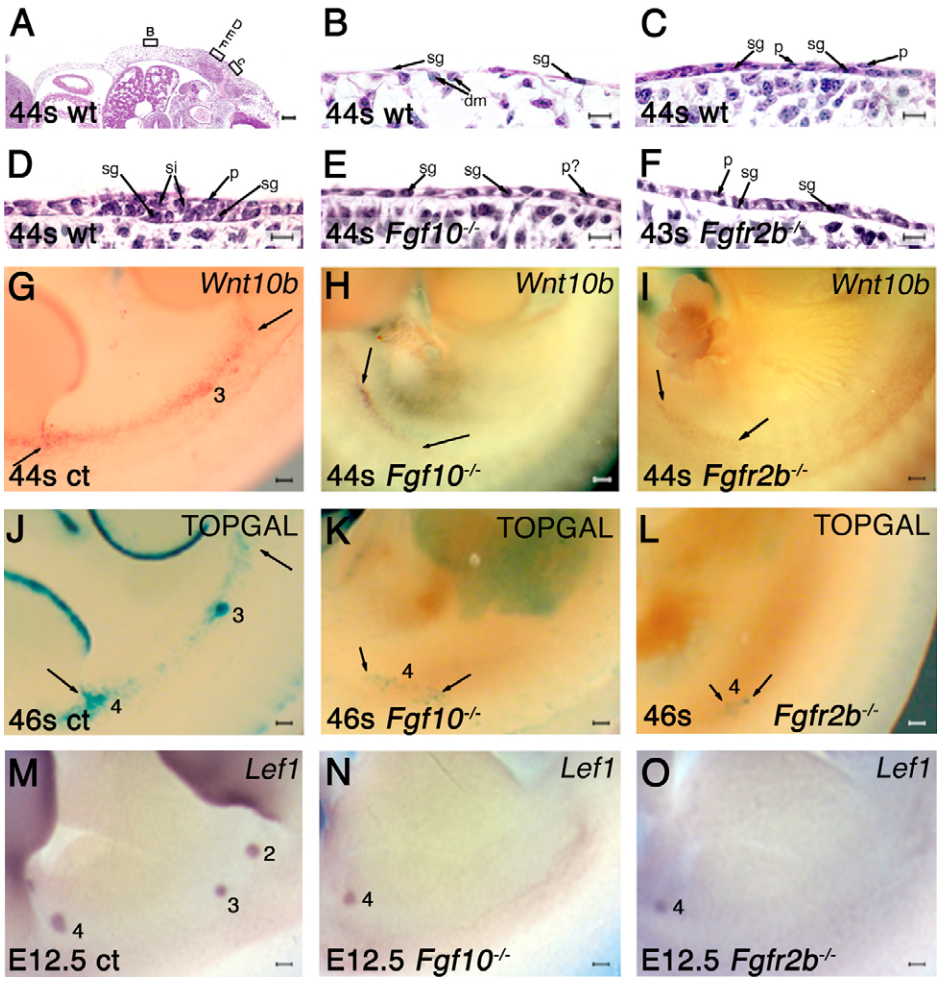

Fig. 3. Impaired mammary line formation precedes the absence of mammary placodes in *Fgf10*$^{-/-}$ and *Fgfr2b*$^{-/-}$ embryos.
(**A-F**) Hematoxylin/Eosin-stained sections through a wild-type (A-D), *Fgf10*$^{-/-}$ (E) and *Fgfr2b*$^{-/-}$ embryo (F) around E11.5, through the plane indicated by the line in Fig. 2E. Boxed areas in A are magnified in B-F. First, the stratum germinativum consists of squamous cells (B) that become cuboidal and covered with a layer of periderm (C) on the Wolffian ridge or flank. Next, they become cylindrical and form an additional layer (stratum intermedium) of cylindrical cells on the ventral area of the flank (D). This indicates mammary line formation, which does not occur in either mutants (E,F). (**G-I**) In situ hybridization for *Wnt10b* expression shows formation of the mammary line (between arrows) and mammary placodes (numbered), restricted to the area of placode 4 in the mutants. (**J-L**) X-gal staining visualizing TOPGAL expression indicates that WNT signaling occurs in a pattern similar to *Wnt10b* expression. (**M-O**) In situ hybridization for *Lef1* reveals that all placodes (numbered) except 4 are absent in the mutants. Abbreviations: s, somite stage; wt, wild type; ct, control; sg, stratum germinativum; dm, dermal mesenchyme; p, periderm; si, stratum intermedium. Scale bars: 10 μm in B-F; 100 μm in G-O; 1 mm in A.

By E10.5, hypaxial *Fgf10* expression has descended to thoracic somites 17-18 (Mailleux et al., 2002), which lie just posterior to the prospective mammary placode 3 (Eblaghie et al., 2004) (J.M.V., unpublished). Using the more sensitive radioactive in situ hybridization, we detected *Fgf10* mRNA in the hypaxial buds and at a lower level throughout the somites from E10.5 onwards, shown for E10.75 (37 somites) (Fig. 4C), but not in the dermal mesenchyme and surface ectoderm. By E11.5, when placode 3 has formed, *Fgf10* expression has increased throughout the somites, and is still relatively high in the hypaxial buds (Fig. 4D). A radioactive signal above background levels in the dermal mesenchyme suggests that *Fgf10*-expressing cells delaminate from the somites. While the mammary placodes transform into buds, somitic *Fgf10* expression becomes progressively reduced [data not shown at E12.0 (50 somites) and E12.5 (54 somites)]. These data support a role for hypaxial and central somitic *Fgf10* expression from around E10.5 onwards in the induction of a mammary cell fate.

Fgfr2b mRNA was detected in the surface ectoderm at E9.5 (26s) and during the onset of mammary line formation at E11.0 (41s), but not in the somites and dermal mesenchyme (Fig. 4E-H). No expression of any other Fgfr isoform was detected in the somites, dermal mesenchyme or ectoderm at these stages (not shown). Notably, *Fgfr2b* expression is relatively high in the surface ectoderm overlying the hypaxial buds at E11.5-E12.25 (45-50 somites) (Fig. 4G,H), corresponding to the area of the mammary line. These expression data support the hypothesis that somitic FGF10 acts via ectodermal FGFR2B in mammary line formation, prior to placode formation. However, it is still possible that *Fgf10* expression in the lateral plate mesoderm at E9.5-10 makes the ectoderm receptive to later somitic signals involved in mammogenesis.

Recombinant FGF10 rescues placode formation in *Fgf10*$^{-/-}$ embryos

To address the latter possibility, we dissected the flanks including a small piece of ventral skin of E11.5 and E12.5 wild-type and *Fgf10*$^{-/-}$ embryos. These explants were completely eviscerated, to comprise only the skin and somites, and included the limbs in the case of a wild type. The flanks were cultured for 2 or 3 days with a bead soaked in BSA or recombinant FGF10 (rFGF10) implanted on the hypaxial buds of somites 14-15 or 17-18, just anterior or posterior to the position where placode 3 normally develops.

In wild-type flanks without bead or with a BSA bead (Fig. 4I), we either found no, one, two or occasionally all three buds (2, 3 and 4) expected between the limbs (Table 1), as assessed by *Wnt10b* (Fig. 4I-L) or TOPGAL expression. Implantation of an rFGF10 bead in wild-type flanks (Fig. 4K) or a BSA bead in *Fgf10*$^{-/-}$ flanks (Fig. 4J) never resulted in the formation of a supernumerary mammary rudiment. Remarkably, in 30% of *Fgf10*$^{-/-}$ flanks cultured with an rFGF10 bead, we detected one bud in addition to the only bud (4) that normally forms in these mutants, by *Wnt10b* expression and histology (Fig. 4L-N). Although rFGF10 failed to induce extra placodes in wild-type flanks, the rescue of bud formation in *Fgf10*$^{-/-}$

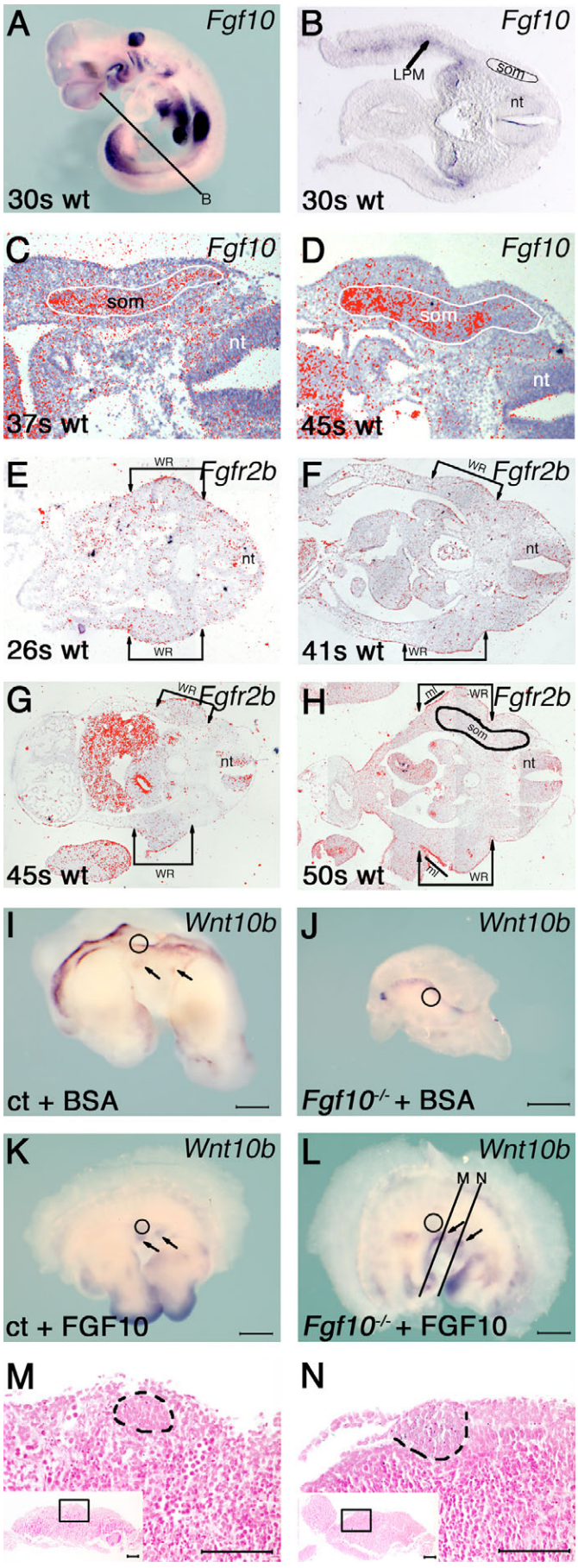

Fig. 4. *Fgf10* and *Fgfr2b* expression patterns and rescue of the *Fgf10*$^{-/-}$ mammary defect by recombinant FGF10. (**A**,**B**) In situ hybridization for *Fgf10* on an E10.0 (30 somite) wild-type embryo; whole-mount (A) and a 40 μm vibratome section (B) along the plane indicated by the line in A. *Fgf10* expression is present in the lateral plate mesoderm of the flank. (**C-H**) Radiolabeled in situ hybridization on Hematoxylin counterstained sections shows *Fgf10* expression (red) in the somites (white contours in C,D), and *Fgf2b* expression (red) in the surface ectoderm (E-H). The arrowed brackets in E-H indicate the Wolffian ridge (WR) or flank. The mammary line (ml) overlying the hypaxial bud of the somite (black contour in H) expresses elevated levels of *Fgfr2b*. (**I-L**) Whole-mount in situ hybridization for *Wnt10b,* showing mammary placode formation (arrows) in a flank of a control (I,K) or *Fgf10*$^{-/-}$ embryo (J,L), cultured with an implanted bead (circle) soaked in BSA (I,J) or rFGF10 (K,L). (**M**,**N**) Nuclear Fast Red stained section at the level of the lines through the flank in L. Boxed area in the insets are magnified; broken black lines outline the placodes. Abbreviations: LPM, lateral plate mesoderm; nt, neural tube; s, somite stage; som, somite; WR, Wolffian ridge; ml, mammary line. Panels A-H are not to scale. Scale bars: 1 mm in I-L; 100 μm in M,N.

explants of fairly advanced stages (E11.5 and even E12.5) indicates that the initiation of mammogenesis does not depend on *Fgf10* expression prior to somitic *Fgf10* expression.

Impaired mammogenesis correlates with reduced somitic *Fgf10* expression in *Gli3*$^{Xt\text{-}J/Xt\text{-}J}$ embryos

The *Gli3*$^{Xt\text{-}J}$ mutation represents a functional null allele for the transcription factor GLI3 (Maynard et al., 2002). *Gli3*$^{Xt\text{-}J/Xt\text{-}J}$ embryos lack mammary bud 3 at E13.5 (Johnson, 1967). In the wild-type mouse embryo, *Gli3* is expressed in the somites (McDermott et al., 2005), and GLI and FGF family members genetically interact in organogenesis (Brewster et al., 2000; Aoto et al., 2002; te Welscher et al., 2002; Kuschel et al., 2003). Therefore, we examined whether the bud defect is preceded by impaired initiation of mammogenesis in *Gli3*$^{Xt\text{-}J/Xt\text{-}J}$ embryos, and whether initiation of mammogenesis required an interaction between somitic *Fgf10* and *Gli3*.

Wnt10b and TOPGAL expression are reduced at the level of the mammary line, and not elevated at the position of placode 3 in *Gli3*$^{Xt\text{-}J/Xt\text{-}J}$ embryos at E11.5 (44 somite) (Fig. 5A-D). Accordingly, *Lef1* is expressed at the position of mammary buds 2 and 4, but not of bud 3 by E12.5 (Fig. 5E,F). The cells of the stratum germinativum are cylindrical, slightly enlarged along the width of the mammary line and, as in *Pax3*$^{ILZ/ILZ}$ mutants and wild-type embryos, covered with periderm. However, the stratum intermedium is absent (Fig. 5G,H), in accordance with the reduced expression levels of *Wnt10b* and TOPGAL, and absence of *Lef1* expression. Thus, mammary line formation is indeed impaired in *Gli3*$^{Xt\text{-}J/Xt\text{-}J}$ embryos. In contrast to the delayed formation of placode 3 in *Pax3*$^{ILZ/ILZ}$ mutants, gland 3 was not found at all in histological sections or skin preparations of *Gli3*$^{Xt\text{-}J/Xt\text{-}J}$ embryos between E12.5 and term (not shown).

In situ hybridization revealed high *Gli3* expression in all thoracic somites at E10.0-E11.0 (whole-mount data not shown; Fig. 5I). *Gli3* is less expressed in the dermal mesenchyme, and not detected in the surface ectoderm. *Gli3* expression is normal in the somites of E10.5-E11.5 *Fgf10*$^{-/-}$ embryos (Fig. 5J,K). Conversely, *Fgf10* expression is not detected in the central somitic domain, and reduced in the hypaxial somitic domain of E10.5-E11.5 *Gli3*$^{Xt\text{-}J/Xt\text{-}J}$ embryos. Moreover, *Fgf10* expression extends posteriorly to only the level of somite 16 instead of 18 in *Gli3*$^{Xt\text{-}J/Xt\text{-}J}$ embryos (Fig. 5L,M).

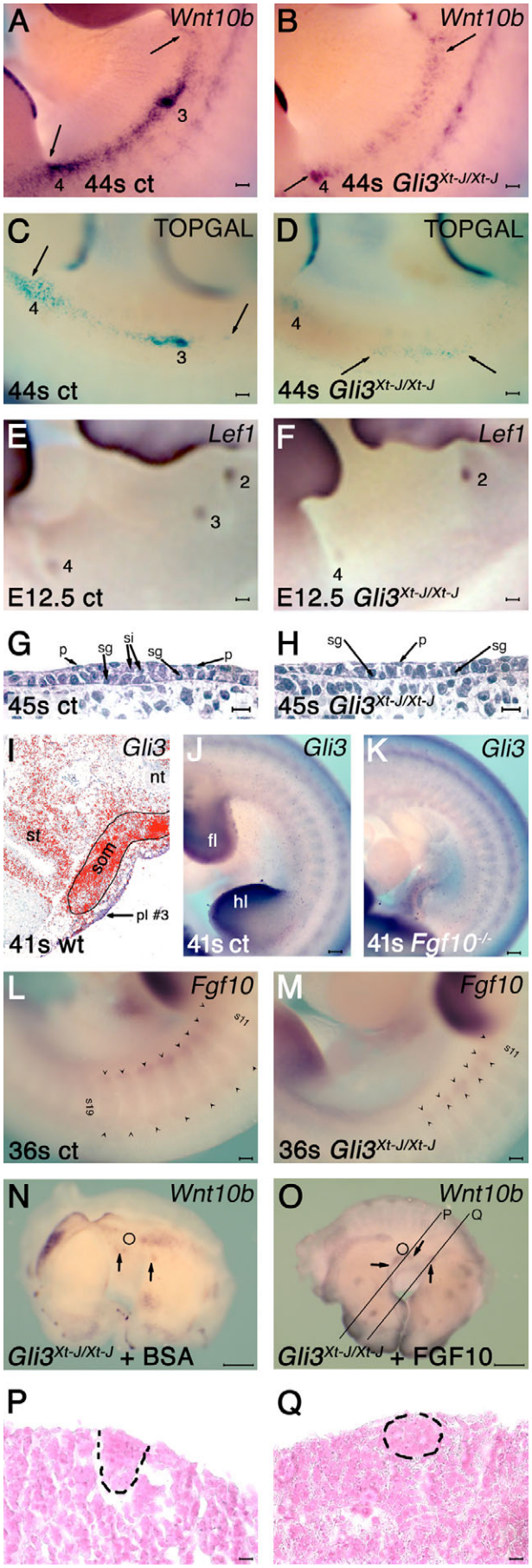

Fig. 5. Impaired mammary line formation due to reduced somitic *Fgf10* expression precedes the absence of mammary bud 3 in *Gli3*$^{Xt\text{-}J/Xt\text{-}J}$ embryos. (**A**,**B**) Whole-mount in situ hybridization for *Wnt10b* reveals impaired mammary line formation (between arrows), the presence of placodes 2 and 4 (numbered), but not placode 3 in an E11.5 (44s) *Gli3*$^{Xt\text{-}J/Xt\text{-}J}$ embryo. (**C**,**D**) X-gal staining for TOPGAL expression indicates that WNT signaling in an E11.5 *Gli3*$^{Xt\text{-}J/Xt\text{-}J}$ embryo is reduced in a pattern similar to *Wnt10b* expression. (**E**,**F**) Whole-mount in situ hybridization for *Lef1* reveals the absence of bud 3 in an E12.5 *Gli3*$^{Xt\text{-}J/Xt\text{-}J}$ embryo. (**G**,**H**) Hematoxylin/Eosin-stained sections through the plane indicated in Fig. 2E reveals the absence of the stratum intermedium at the mammary line of an E11.5 (45 somites) *Gli3*$^{Xt\text{-}J/Xt\text{-}J}$ mutant. (**I-K**) Radiolabeled in situ hybridization for *Gli3* (red) on a section of an E11.0 (41 somite) wild-type embryo (I) through the plane indicated in Fig. 2E, and whole-mount in situ hybridization for *Gli3* on a control (J) and *Fgf10*$^{-/-}$ (K) embryo shows unchanged somitic *Gli3* expression in the *Fgf10*$^{-/-}$ mutant. (**L**,**M**) Whole-mount in situ hybridization for *Fgf10* reveals that somitic *Fgf10* expression (between black arrowheads) is restricted to the hypaxial domain in the *Gli3*$^{Xt\text{-}J/Xt\text{-}J}$ embryo. (**N**,**O**) Whole-mount in situ hybridization for *Wnt10b* on flanks of *Gli3*$^{Xt\text{-}J/Xt\text{-}J}$ embryos, cultured with an implanted bead (circle) soaked in BSA (N) or rFGF10 (O). Arrows indicate the mammary placodes or the expansion of a *Wnt10b* expression domain around the bead in O. (**P**,**Q**) Nuclear Fast Red stained section through the planes indicated by lines through the flank in L. Broken black lines outline the mammary epithelium. Abbreviations: s, somite stage; p, periderm; sg, stratum germinativum; si, stratum intermedium; pl #3, mammary placode 3; nt, neural tube; st, stomach; fl, forelimb; hl, hindlimb; rFGF10, recombinant FGF10. Scale bars: 10 μm in G-H,P-Q; 100 μm in A-F,I-M; 1 mm in N,O. Panel I is not to scale.

Furthermore, hypaxial *Fgf10* expression is highest in somites 15-16, underlying mammary placode 3 in control embryos, whereas it is barely detectable in those somites of *Gli3*$^{Xt\text{-}J/Xt\text{-}J}$ embryos. As patterning and histology of *Gli3*$^{Xt\text{-}J/Xt\text{-}J}$ somites seem normal (McDermott et al., 2004) (our data not shown), the reduced *Fgf10* expression does most probably not reflect an absence of somitic tissue, but is due to an absence of *Gli3* expression.

Implantation of an rFGF10 bead in eleven cultured *Gli3*$^{Xt\text{-}J/Xt\text{-}J}$ flanks resulted once in an extended streak of *Wnt10b* expression and thickened ectoderm (Fig. 5O,P; Table 1). Given the low frequency of normal placode development in control explants (8/70, see Table 1), this extension may indicate a rescue of formation of the mammary line and placode 3. We conclude that *Gli3* expression is required to maintain high levels of *Fgf10* expression along the dorsoventral gradient within somites 12-18, and the anteroposterior *Fgf10* gradient across these somites, which is in turn required for the complete formation of the mammary line and placode 3.

Hypomorphic Fgf10 mutants lack placode 3

To test whether reduced *Fgf10* expression is indeed responsible for the mammary phenotype in *Gli3*$^{Xt\text{-}J/Xt\text{-}J}$ embryos, we generated embryos carrying one *Fgf10*$^{-}$ allele and one *Fgf10*^{mlcv} allele (Kelly et al., 2001), which expresses reduced levels of *Fgf10* (Mailleux et al., 2005). This allelic combination results in a hypomorphic *Fgf10* phenotype in the embryonic lung (Mailleux et al., 2005), limbs (arrows in Fig. 6D,F) and gut (F.G.S., J. L. Curtis, J.M.V., P. M. Del Moral, T. Fairbanks, D. Warburton, K. Wang, R. C. Burns and S.B., unpublished). The mammary line does form in these embryos, and so do mammary placodes 2 and 4. However, we could neither detect

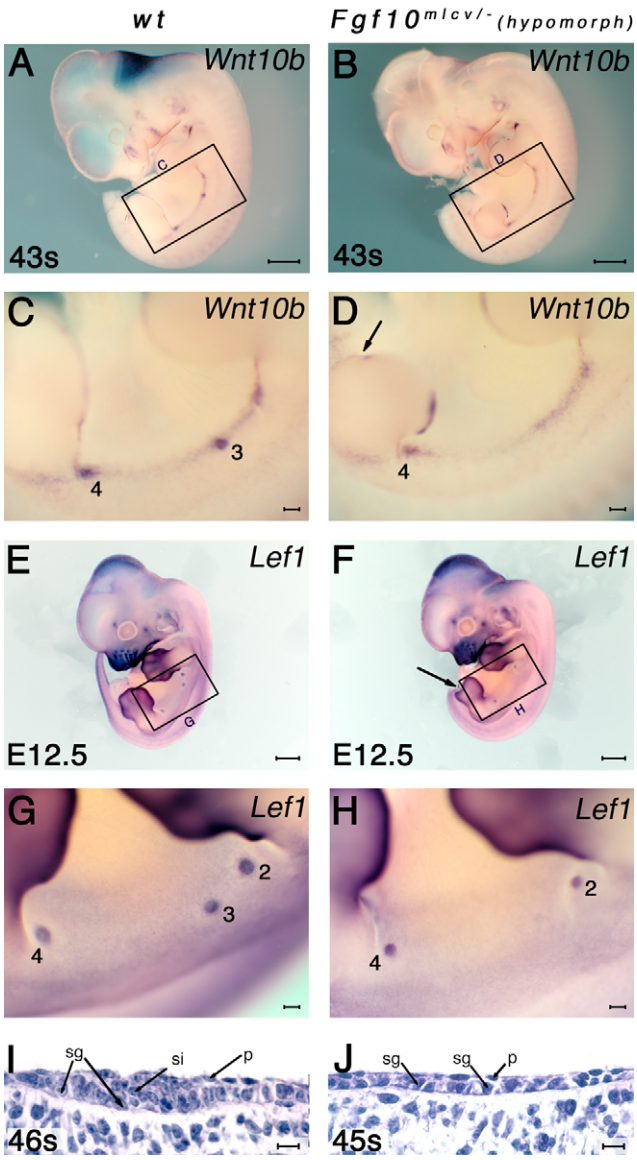

Fig. 6. Hypomorphic *Fgf10* mutants phenocopy the mammary defect of *Gli3*$^{Xt\text{-}J/Xt\text{-}J}$ embryos. Boxed areas in A,B,E,F are shown at high magnification in C,D,G,H. (**A-D**) Whole-mount in situ hybridization for *Wnt10b* reveals the absence of placode 3 in an E11.25 (43 somite) *Fgf10* hypomorphic (*Fgf10*$^{mlcv/-}$) mutant. (**E-H**) Whole-mount in situ hybridization for *Lef1* reveals the absence of bud 3 in an E12.5 *Fgf10* hypomorphic mutant. (**I,J**) Hematoxylin/Eosin-stained sections, showing the absence of the stratum intermedium in an E11.5 (45 somite) mutant. Arrows in D and F indicate morphological limb defects in *Fgf10* hypomorphic mutants, while limbs are totally absent in *Fgf10*$^{-/-}$ embryos. Abbreviations: sg, stratum germinativum; p, periderm; s, somite stage. Scale bars: 10 μm in M,N; 100 μm in C,D,G,H; 1 mm in A,B,E,F.

placode 3 in E11.5 and E12.5 hypomorphs by *Wnt10b* and *Lef1* expression (Fig. 6A-H), nor in histological sections of embryos until term (not shown). Along the mammary line, cells of the stratum germinativum are still cuboidal at E11.0 (40 somites) instead of cylindrical and covered by periderm (not shown). By E11.5 (45 somites) cells of the stratum germinativum are also enlarged cylindrical in hypomorphs, and covered by periderm as in control embryos, but fail to generate a stratum intermedium (Fig. 6I,J). The mammary phenotype of hypomorphs is thus less severe than that of *Fgf10*$^{-/-}$ mutants and very similar to that of *Gli3*$^{Xt\text{-}J/Xt\text{-}J}$ mutants, while the absence of rudiment 3 distinguishes this phenotype from that of *Pax3*$^{ILZ/ILZ}$ embryos. These data strongly support the conclusion that reduced somitic *Fgf10* expression impairs mammary line formation and abolishes formation of placode 3 in *Gli3*$^{Xt\text{-}J/Xt\text{-}J}$ embryos.

DISCUSSION

Anterior thoracic somitic Fgf10 expression is required for the initiation of a mammary cell fate

Our study concerned the role of somitic signals, in particular of FGF10, in the initiation of mammary development. With the *Pax3* mutant data, we showed that in the absence of hypaxial signals, placode 3 develops late and remains hypoplastic, while the other placodes develop apparently normal. This differential requirement of placodes for hypaxial somitic signals reflects their differential requirement for total somitic FGF10 (see Table 2). Mammary placode 3 is most sensitive to reduced somitic FGF10 expression, as found in *Gli3*$^{Xt\text{-}J/Xt\text{-}J}$ and *Fgf10* hypomorphic mutants, in accordance with the highest hypaxial *Fgf10* expression found in somites 15 and 16 underlying this placode in wild-type embryos; placodes 1, 2 and 5, though requiring FGF10/FGFR2B signaling, develop in the presence of reduced somitic FGF10 expression in *Pax3*$^{ILZ/ILZ}$, *Gli3*$^{Xt\text{-}J/Xt\text{-}J}$ and *Fgf10* hypomorphic mutants; placode 4 does not require FGF10 or FGFR2B at all for its formation. With the *Pax3* mutant data, we also correlated the position of the ventral edge of the thoracic somites with the position of the mammary line on the dorsoventral axis of the flank. We now conclude that hypaxial somitic FGF10 is required for the correct dorsoventral positioning of the mammary line, and additional central somitic FGF10 is required for the formation of placode 3 on the anteroposterior aspect of this line. We present here the first evidence that slight modulations in levels and localization of gene expression, regulating interactions between the somites and the flank surface ectoderm, determine epidermal versus mammary cell fate decisions in, and thus patterning of, this ectoderm.

Identification of a GLI3-FGF10/FGFR2B-WNT signaling cascade, required for induction of the mammary cell fate at the position of mammary placode 3

Fgf10 expression is reduced in the somites in *Gli3*$^{Xt\text{-}J/Xt\text{-}J}$ mutants, indicating that GLI3 acts upstream of *Fgf10* (Fig. 7A). We have observed the same genetic interaction in lambdoid suture formation (R.R., E. Connor, J.M.V., E. Lana-Elola, S.B. and D.P.R., unpublished). To our knowledge, this is the first time that any GLI function has been placed upstream of FGF10. GLI3 is a transcriptional activator or repressor dependent on the level of Hedgehog signaling (Lewis and Veltmaat, 2004; Stamataki et al., 2005). GLI3 exerts an activator function in the epaxial-medial domain of the somites, and a repressor function in the lateral domain of the somites (McDermott et al., 2005). GLI3 may therefore directly or indirectly activate *Fgf10* transcription in somitic subdomains. No GLI-binding sequence has been found within 6.6 kb upstream of the *Fgf10*-coding sequence (Ohuchi et al., 2005). However, sequences further upstream, e.g. as far as 114 kb (Kelly et al., 2001; Mailleux et al., 2005), may contain regulatory elements including GLI3-binding sites. Interestingly, null mutants for sonic hedgehog form all mammary placodes (Gallego et al., 2002; Michno et al., 2003), indicating that sonic hedgehog is not required for GLI3-mediated activation of *Fgf10* transcription.

Table 1. Recombinant FGF10 rescues placode formation in vitro

Number of glands	Genotype and treatment: Control	Control + BSA	Control + *Fgf10*	*Fgf10*$^{-/-}$ + BSA	*Fgf10*$^{-/-}$ + *Fgf10*	*Gli3*$^{Xt\text{-}J/Xt\text{-}J}$	*Gli3*$^{Xt\text{-}J/Xt\text{-}J}$ + BSA	*Gli3*$^{Xt\text{-}J/Xt\text{-}J}$ + *Fgf10*
0	5	4	27	2	10	1	0	6
1	0	6	4	0	6	0	0	1
2	0	6	7	0	7*	1	1	3
3	2	2	2	0	0	0	0	1*

Total number of explants: 104

Row 1 lists the genotypes of the flanks cultured with either no bead implanted, or with a bead soaked in BSA or rFGF10. Column 1 lists the total number of developing glands in these flanks as observed by *Wnt10b* or TOPGAL expression. The body of the table lists the number of flanks in which gland formation was analyzed.
*rFGF10 induced a supernumerary rudiment in ~30% (7/23) of *Fgf10*$^{-/-}$ flanks and 9% (1/11) of *Gli3*$^{Xt\text{-}J/Xt\text{-}J}$ flanks, but never in flanks of control embryos.
Abbreviations: n.d., not determined; rFGF10, recombinant FGF10.

We also show that *Wnt10b* expression and canonical WNT signaling are activated downstream of FGF10/FGFR2B signaling in the surface ectoderm (Fig. 7A), and thus identified a genetic cascade from GLI3 via FGF10/FGFR2B to *Wnt10b* expression, and to canonical WNT signaling required for the induction of a mammary cell fate in the ectoderm. *Wnt10b* expression precedes TOPGAL expression, and coincides with the acquisition of an enlarged cylindrical cell shape (Fig. 5H, Fig. 6J). Both *Wnt10b* and TOPGAL expression increase with localized multilayering of the flank ectoderm. Multilayering is initially restricted to the mammary line. Previously, the enlargement of cells of the single-layered ectoderm was suggested to indicate mammary line formation (Turner and Gomez, 1933; Sakakura, 1987). Although enlargement of cylindrical cells coincides with low levels of *Wnt10b* expression, it is not sufficient for the formation of a mammary placode, as seen in *Gli3*$^{Xt\text{-}J/Xt\text{-}J}$ and hypomorphic *Fgf10* mutants. Therefore, we postulate that multilayering is the first histological manifestation of a mammary cell fate.

A model combining ventral elongation of the thoracic somites with gradients of somitic Fgf10 expression in the patterning of mammary epithelium in the interlimb region

Based on the similarity in mammary phenotype of *Fgf10*$^{-/-}$ and *Fgfr2b*$^{-/-}$ mutants (Table 2), and on the complementary expression patterns of *Fgf10* and *Fgfr2b* in wild-type embryos, we conclude that somitic FGF10 binds to and activates ectodermal FGFR2B, leading to a mammary cell fate in the ectoderm. An analysis of transverse sections at the level of somites 14-18 of progressively older wild-type embryos revealed that the prospective hypaxial buds of the thoracic somites are located dorsal to the flank at E10.0 (30 somites). The somites extend ventrally, growing into the lateral plate mesoderm of the flank between E10.5 and E11.5 (35-45 somites). Elongating more rapidly than the dorsoventral axis of the body, they reach the ventral side of the flank by E12.0 (50 somites). We observed that the ectodermal cell morphology changes from cuboidal to cylindrical along the dorsoventral axis of the flank during somitic elongation. Subsequently, the cylindrical cells enlarge, express *Wnt10b* (Fig. 5B,H) and give rise to the stratum intermedium. This enlargement and multilayering occurs first at the ventral position of the flank between E11 and E11.5, where it indicates mammary line formation. Somitic elongation also coincides with the onset of somitic *Fgf10* expression (pink in Fig. 7B, based on Fig. 4A-D and data not shown). Therefore, somitic FGF10 may mediate ectodermal maturation even before the differentiation into mammary epithelium. The cuboidal morphology of the ectodermal cells in *Fgf10*$^{-/-}$ and *Fgfr2b*$^{-/-}$ mutants (Fig. 3E,F) demonstrates that FGF10/FGFR2B signaling is not required for the maturation of squamous ectoderm cells into cuboidal cells. However, it is required for the progression to a cyclindrical ectodermal cell shape. In *Gli3*$^{Xt\text{-}J/Xt\text{-}J}$ and hypomorphic *Fgf10* mutants, the somites elongate normally, but express reduced levels of *Fgf10*. This correlates with the acquisition of an enlarged cylindrical cell morphology and low levels of *Wnt10b* expression, yet failure to form the stratum intermedium by E11.5 (Fig. 5H,

Table 2. Correlation between somitic *Fgf10* expression and mammary development

Genotype	*Fgf10* expression in somitic subdomains	Histology of mammary line at E11.5 (±45 seconds)	Development of mammary placodes: 1	2	3	4	5
Wild type	Entire somites 11-18, high hypaxial and epaxial expression	Cylindrical s.g., cylindrical s.i., covered with periderm	+	+	+	+	+
Pax3$^{ILZ/ILZ}$	No hypaxial and epaxial expression, normal central expression in somites 11-18	Cylindrical s.g., reduced cylindrical s.i., covered with periderm	+	+	Late	+	+
Fgf10$^{-/-}$	None	Cuboidal s.g., no s.i., periderm impaired	–	–	–	+	–
Fgfr2b$^{-/-}$	As wild type (absent receptor for somitic FGFf10)	As *Fgf10*$^{-/-}$	–	–	–	+	–
Gli3$^{Xt\text{-}J/Xt\text{-}J}$	Only hypaxial somites 11-16, low expression levels	Cylindrical s.g., no s.i., covered with periderm	+	+	–	+	–
Fgf10^{hypomorph}	Pattern as in wild type, but lower expression levels	As *Gli3*$^{Xt\text{-}J/Xt\text{-}J}$	+	+	–	+	+

For each mutant used in this study (column 1), the *Fgf10* expression pattern in the somites (column 2) and the histology of the mammary line at around E11.5 (column 3) are described. The formation (+) or the absence (–) of each of the five placode pairs is also indicated (columns 4-8).
Abbreviations: s.g., stratum germinativum; s.i., stratum intermedium.

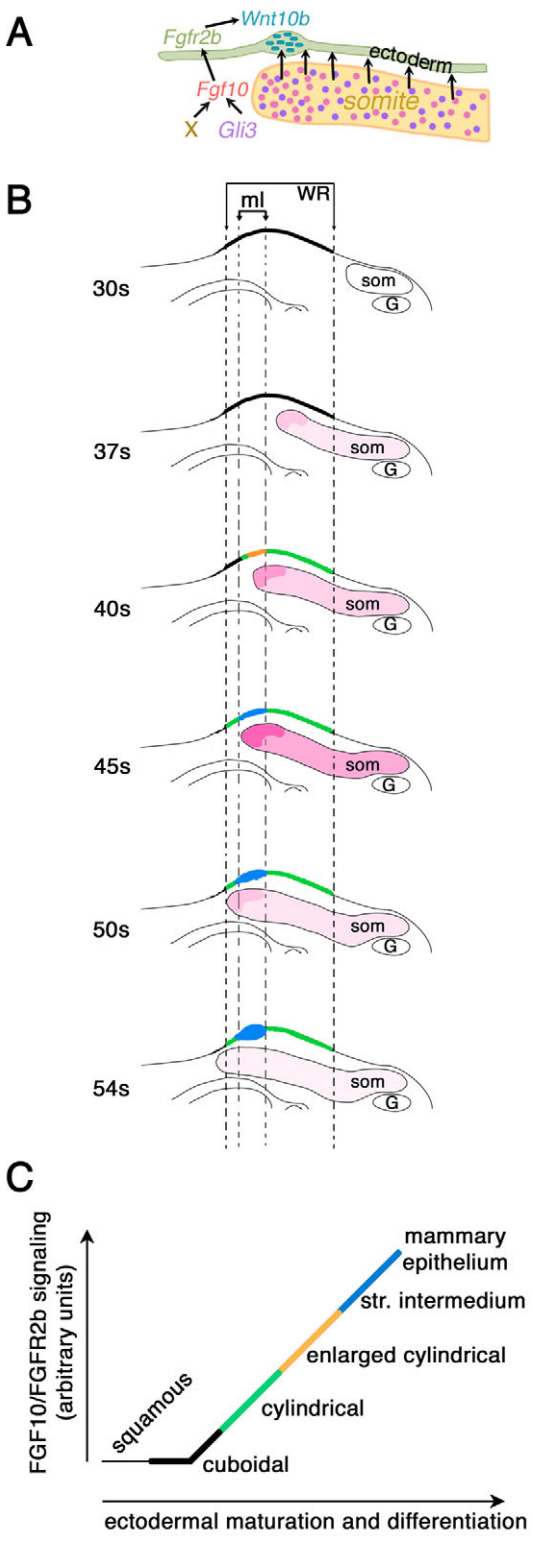

Fig. 7. A model combining ventral elongation of the somites and somitic *Fgf10* expression with maturation of the surface ectoderm and the acquisition of a mammary cell fate at the position of mammary placode 3. (**A**) A model for the molecular interactions leading to a mammary cell fate in the surface ectoderm. GLI3 (purple dots) and an unidentified factor or factors X act upstream of *Fgf10* (pink dots) in the somites. Somitic FGF10 activates ectodermal FGFR2B (green), via diffusion and/or delamination of somitic cells. Sufficient levels of activation are required for *Wnt10b*/TOPGAL expression (blue) and multilayering of the surface ectodermal cells as hallmarks of a mammary cell identity. (**B**) Schematic drawings of body halves of progressively older embryos, illustrating the correlation between somitic elongation, somitic *Fgf10* expression and ectodermal maturation. For convenience, the body size is kept the same for all ages. Broken vertical lines indicate the mammary line (ml) and Wolffian ridge (WR). Increasingly darker shades of pink indicate increasingly higher levels of *Fgf10* expression. The surface ectodermal cells are cuboidal (thicker black line) at the WR, whereas dorsal and ventral to the WR they are squamous (thinner black line). Ventrally on the flank, ectodermal cells become cylindrical (green) and enlarge (orange) coinciding with low levels of *Wnt10b* and TOPGAL expression. These cells give rise to a stratum intermedium (blue), with elevated *Wnt10b* and TOPGAL expression, indicating a mammary cell fate. (**C**) Model of cumulative FGF10/FGFR2B signaling in the flank leading to progressive maturation of the ectoderm, and eventually conversion into mammary epithelium. See main text for explanation. Color coding corresponds to color coding of B. Abbreviations: G, dorsal root ganglion; som, somite.

Fig. 6J). Therefore, we conclude that progressive maturation of the ectoderm requires increasing amounts of somitic FGF10 (Fig. 7C).

Hypaxial somitic *Fgf10* expression is absent, while central somitic *Fgf10* is expressed at normal levels in $Pax3^{ILZ/ILZ}$ mutants. In these mutants, the stratum intermedium is being formed at E11.5 (Fig. 2P), suggesting that total somitic *Fgf10* expression is higher than in $Gli3^{Xt\text{-}J/Xt\text{-}J}$ and hypomorphic *Fgf10* mutants. In contrast to the latter two mutants, $Pax3^{ILZ/ILZ}$ mutants form placode 3, albeit delayed and hypoplastic. The profile and dynamics of somitic *Fgf10* expression may explain this phenotype: in wild-type embryos, *Fgf10* is expressed from E10.5 onwards, at a higher level in the hypaxial bud than in the central somitic compartment. Expression increases throughout the entire somite between E10.5 and E11.5, during which time the mammary line and placode 3 are formed. It decreases but remains present towards E12.5 (Fig. 4C,D and Fig. 7B). This prolonged *Fgf10* expression may compensate for the absence of hypaxial *Fgf10* in $Pax3^{ILZ/ILZ}$ mutants, and allow the ectoderm to complete its maturation and differentiation into mammary epithelium. By contrast, central somitic *Fgf10* expression in $Gli3^{Xt\text{-}J/Xt\text{-}J}$ and *Fgf10* hypomorphic mutants is too low to provide a similar compensatory mechanism. This suggests that the total amount of FGF10 signaling via FGFR2B, accumulated during a prolonged period of time rather than during a short moment, determines the formation of mammary epithelium.

The absence of the ventral bud of the somites correlates with a more dorsal location of the mammary line in $Pax3^{ILZ/ILZ}$ mutants. As the line is located above the ventral-most edge of the somite, we conclude that the position of the mammary line is determined by the ventral edge of the thoracic somites, or ventral-most delivery point of somitic FGF10, rather than being predetermined in the ectoderm and waiting for FGF10 signals. In summary, we propose that the intra-somitic *Fgf10* expression gradient and dynamics, combined with the rapid hypaxial elongation of the thoracic somites, determines the dorsoventral position of the mammary line and the progressive differentiation towards a mammary cell fate at the position of placode 3 on the anteroposterior aspect of this line.

Delaminating epaxial and central somitic dermomyotomal cells form the dorsal dermis before E11 in the mouse (Houzelstein et al., 2000). Some of these cells may mix with the flank mesenchyme at the dorsolateral boundary, as shown in chick (Olivera-Martinez et

al., 2000; Nowicki et al., 2003). Although it remains to be elucidated whether somitic FGF10 reaches the overlying ectoderm by a similar delamination of dermal precursors, or by diffusion, or by both mechanisms, we provide evidence that somitic FGF10 is required for the earliest differentiation steps of the ectoderm, and subsequently for the formation of mammary epithelium. To our knowledge, this is the first evidence that the hypaxial and central domain of the somites are implicated in the differentiation and patterning of the flank ectoderm. The failure of cells of the stratum germinativum to become cylindrical and generate a stratum intermedium in E11.5 *Fgfr2b*$^{-/-}$ and *Fgf10*$^{-/-}$ mutants may underlie the hypoplasia of the stratum granulosum [derived from the stratum germinativum and intermedium (Sengel, 1976)] observed in these mutants at birth, and the impaired hair follicle formation in *Fgfr2b*$^{-/-}$ but not in *Fgf10*$^{-/-}$ mutants (Suzuki et al., 2000; Petiot et al., 2003).

Does FGF10 regulate epithelial migration during the initiation of mammogenesis?

The mammary line and placodes show an increased cell density compared with the surrounding ectoderm. As this density seems to be established without locally increased cell proliferation, it has been suggested that cells migrate towards and along the mammary line (Balinsky, 1949-1950). Although cells have never been shown experimentally to migrate along the mammary line, the observation of elongated, fibroblast-like morphology of cells along the mammary line may indeed suggest migratory behavior of these cells (Propper, 1978; Chu et al., 2004). This view may be supported by the fragmented *Wnt10b* expression domain on the flank, fusing into one continuous mammary line (Veltmaat et al., 2003), and by the transition of a small stripe of *Lef1* expression into a dot via a comet-shaped intermediate at the level of placode 3 (Mailleux et al., 2002). It now raises the interesting issue of whether FGF10 mediates cell migration during mammary line and placode formation, as it does in eyelid development (Tao et al., 2005) and lung development (Bellusci et al., 1997; Park et al., 1998). In this scenario, cells along the flank would be pulled in a ventral direction along with the elongating hypaxial buds. As *Fgf10* expression is highest in the hypaxial buds of somites 15 and 16, *Wnt10b*-expressing cells along the mammary line would be recruited to the position above these somites to form placode 3. Such recruitment is supported by the condensation of initially three fragments of high *Wnt10b* expression somites 15, 16 and 17, to one continuous domain above somite 15 and 16 (Veltmaat et al., 2004). The shorter somites in *Pax3*$^{ILZ/ILZ}$ mutants would draw ectodermal cells across a narrower, more dorsal domain, resulting in a more dorsal position of the mammary line. In combination with reduced production of total somitic FGF10, fewer ectodermal cells would be recruited, leading to a narrower line and delayed multilayering. Subsequently, the absence of the high hypaxial *Fgf10* expression of somites 15 and 16 would then explain why *Wnt10b* expression remains present for a prolonged period along the mammary line, instead of coalescing at the position of placode 3.

Does mammogenesis depend on a unique molecular network for the induction of each pair of placodes?

Little is known about the initiation of mammogenesis, and less is known about the sources of molecules used in the formation of the five individual placode pairs. We show here that placode 3 is most sensitive to a reduction of somitic *Fgf10*. Similarly, placode 3 is more sensitive than placodes 2 and 4 to loss of *Gli3* (this report) or neuregulin 3 (Howard et al., 2005). Gland 3 is also the gland most frequently absent in wild-type mice (Little and McDonald, 1945). Furthermore, increased signaling through EDA/EDAR leads to formation of supernumerary placodes only between placode 3 and 4 (Mustonen et al., 2004), while *Lef1*-null and *Tbx2/3* double heterozygous mutants have a more severe placode induction or maintenance defect in the thoracic region than in the inguinal region (van Genderen et al., 1994; Jerome-Majewska et al., 2005). We can therefore conclude that different molecular networks regulate mammogenesis at different levels along the anteroposterior axis, and different developmental thresholds exist for these networks along this axis. This may explain the differences in number and position of glands along the mammary line in different species, and the incidence of supernumerary nipples and breasts found in 2-5% of the human population (Schmidt, 1998; Grossl, 2000). In particular, with our findings that somitic signals are required for placode formation, we may begin to understand the etiology of Poland's syndrome (Poland, 1841), characterized by compound hypoplasia of the breast and the somite-derived pectoral muscles and thoracic skeletal structures.

Mice were kindly made available to us by Drs Nobuyuki Itoh (*Fgf10*$^{+/-}$), Clive Dickson (*Fgfr2b*$^{+/-}$), John Wysolmerski and Elaine Fuchs (TOPGAL), and Robert Kelly and Margaret Buckingham (*Fgf10*$^{Mlc1v\text{-}nLacZ\text{-}v24}$). We also thank Dr Rudolf Grosschedl for the partial *Lef1* cDNA, Drs D. Dhouailly, Ralf Spörle, Susanne Dietrich and Marek Dudáš for stimulating discussions, and Nicole Rubin for critical reading of the manuscript. We acknowledge financial support from The European Commission/Fifth Framework (QLGA-CT-2000-52130 to J.V.), California Breast Cancer Research Program (9-PB-0082 to S.B. and 10-FB-0116 to J.V.), Childrens Hospital Los Angeles (J.V.), Ellis Fund (K.K.), and the Medical Research Council UK (R.R. and D.R.).

References

Aoto, K., Nishimura, T., Eto, K. and Motoyama, J. (2002). Mouse GLI3 regulates Fgf8 expression and apoptosis in the developing neural tube, face, and limb bud. *Dev. Biol.* **251**, 320-332.

Balinsky, B. I. (1949-1950). On the developmental processes in mammary gland and other epidermal structures. *Trans. R. Soc. Edinb.* **62**, 1-31.

Bellusci, S., Grindley, J., Emoto, H., Itoh, N. and Hogan, B. L. (1997). Fibroblast growth factor 10 (FGF10) and branching morphogenesis in the embryonic mouse lung. *Development* **124**, 4867-4878.

Brewster, R., Mullor, J. L. and Ruiz i Altaba, A. (2000). Gli2 functions in FGF signaling during antero-posterior patterning. *Development* **127**, 4395-4405.

Chu, E. Y., Hens, J., Andl, T., Kairo, A., Yamaguchi, T. P., Brisken, C., Glick, A., Wysolmerski, J. J. and Millar, S. E. (2004). Canonical WNT signaling promotes mammary placode development and is essential for initiation of mammary gland morphogenesis. *Development* **131**, 4819-4829.

DasGupta, R. and Fuchs, E. (1999). Multiple roles for activated LEF/TCF transcription complexes during hair follicle development and differentiation. *Development* **126**, 4557-4568.

De Moerlooze, L., Spencer-Dene, B., Revest, J., Hajihosseini, M., Rosewell, I. and Dickson, C. (2000). An important role for the IIIb isoform of fibroblast growth factor receptor 2 (FGFR2) in mesenchymal-epithelial signalling during mouse organogenesis. *Development* **127**, 483-492.

Eblaghie, M. C., Song, S. J., Kim, J. Y., Akita, K., Tickle, C. and Jung, H. S. (2004). Interactions between FGF and Wnt signals and Tbx3 gene expression in mammary gland initiation in mouse embryos. *J. Anat.* **205**, 1-13.

Eloy-Trinquet, S., Mathis, L. and Nicolas, J.-F. (2000). Retrospective tracing of the developmental lineage of the mouse myotome. In *Somitogenesis Part 1*, Vol. 47 (ed. C. P. Ordahl), pp. 33-80. London: Academic Press.

Gallego, M. I., Beachy, P. A., Hennighausen, L. and Robinson, G. W. (2002). Differential requirements for shh in mammary tissue and hair follicle morphogenesis. *Dev. Biol.* **249**, 131-139.

Grossl, N. A. (2000). Supernumerary breast tissue: historical perspectives and clinical features. *South. Med. J.* **93**, 29-32.

Houzelstein, D., Cheraud, Y., Auda-Boucher, G., Fontaine-Perus, J. and Robert, B. (2000). The expression of the homeobox gene Msx1 reveals two populations of dermal progenitor cells originating from the somites. *Development* **127**, 2155-2164.

Howard, B., Panchal, H., McCarthy, A. and Ashworth, A. (2005). Identification of the scaramanga gene implicates Neuregulin3 in mammary gland specification. *Genes Dev.* **19**, 2078-2090.

Jerome-Majewska, L. A., Jenkins, G. P., Ernstoff, E., Zindy, F., Sherr, C. J. and Papaioannou, V. E. (2005). Tbx3, the ulnar-mammary syndrome gene, and

Tbx2 interact in mammary gland development through a p19(Arf)/p53-independent pathway. *Dev. Dyn*. **234**, 922-933.
Johnson, D. R. (1967). Extra-toes: a new mutant gene causing multiple abnormalities in the mouse. *J. Embryol. Exp. Morphol.* **17**, 543-581.
Kelly, R. G., Brown, N. A. and Buckingham, M. E. (2001). The arterial pole of the mouse heart forms from Fgf10-expressing cells in pharyngeal mesoderm. *Dev. Cell* **1**, 435-440.
Kettunen, P., Karavanova, I. and Thesleff, I. (1998). Responsiveness of developing dental tissues to fibroblast growth factors: expression of splicing alternatives of FGFR1, -2, -3, and of FGFR4; and stimulation of cell proliferation by FGF-2, -4, -8, and -9. *Dev. Genet.* **22**, 374-385.
Kratochwil, K., Galceran, J., Tontsch, S., Roth, W. and Grosschedl, R. (2002). FGF4, a direct target of LEF1 and Wnt signaling, can rescue the arrest of tooth organogenesis in Lef1(–/–) mice. *Genes Dev.* **16**, 3173-3185.
Kuschel, S., Ruther, U. and Theil, T. (2003). A disrupted balance between Bmp/Wnt and Fgf signaling underlies the ventralization of the Gli3 mutant telencephalon. *Dev. Biol.* **260**, 484-495.
Lewis, M. T. and Veltmaat, J. M. (2004). Next stop, the twilight zone: hedgehog network regulation of mammary gland development. *J. Mammary Gland Biol. Neoplasia* **9**, 165-181.
Little, C. C. and McDonald, H. (1945). Abnormalities of the mammae in the house mouse. *J. Hered.* **36**, 285-288.
Mailleux, A. A., Spencer-Dene, B., Dillon, C., Ndiaye, D., Savona-Baron, C., Itoh, N., Kato, S., Dickson, C., Thiery, J. P. and Bellusci, S. (2002). Role of FGF10/FGFR2b signaling during mammary gland development in the mouse embryo. *Development* **129**, 53-60.
Mailleux, A. A., Kelly, R., Veltmaat, J. M., De Langhe, S. P., Zaffran, S., Thiery, J. P. and Bellusci, S. (2005). Fgf10 expression identifies parabronchial smooth muscle cell progenitors and is required for their entry into the smooth muscle cell lineage. *Development* **132**, 2157-2166.
Maynard, T. M., Jain, M. D., Balmer, C. W. and LaMantia, A. S. (2002). High-resolution mapping of the Gli3 mutation extra-toes reveals a 51.5-kb deletion. *Mamm. Genome* **13**, 58-61.
McDermott, A., Gustafsson, M., Elsam, T., Hui, C. C., Emerson, C. P., Jr and Borycki, A. G. (2005). Gli2 and Gli3 have redundant and context-dependent function in skeletal muscle formation. *Development* **132**, 345-357.
Michno, K., Boras-Granic, K., Mill, P., Hui, C. C. and Hamel, P. A. (2003). Shh expression is required for embryonic hair follicle but not mammary gland development. *Dev. Biol.* **264**, 153-165.
Mustonen, T., Pispa, J., Mikkola, M. L., Pummila, M., Kangas, A. T., Pakkasjarvi, L., Jaatinen, R. and Thesleff, I. (2003). Stimulation of ectodermal organ development by Ectodysplasin-A1. *Dev. Biol.* **259**, 123-136.
Mustonen, T., Ilmonen, M., Pummila, M., Kangas, A. T., Laurikkala, J., Jaatinen, R., Pispa, J., Gaide, O., Schneider, P., Thesleff, I. et al. (2004). Ectodysplasin A1 promotes placodal cell fate during early morphogenesis of ectodermal appendages. *Development* **131**, 4907-4919.
Nowicki, J. L., Takimoto, R. and Burke, A. C. (2003). The lateral somitic frontier: dorso-ventral aspects of anterio-posterior regionalization in avian embryos. *Mech. Dev.* **120**, 227-240.
Ohuchi, H., Yasue, A., Ono, K., Sasaoka, S., Tomonari, S., Takagi, A., Itakura, M., Moriyama, K., Noji, S. and Nohno, T. (2005). Identification of cis-element regulating expression of the mouse Fgf10 gene during inner ear development. *Dev. Dyn.* **233**, 177-187.
Olivera-Martinez, I., Coltey, M., Dhouailly, D. and Pourquie, O. (2000). Mediolateral somitic origin of ribs and dermis determined by quail-chick chimeras. *Development* **127**, 4611-4617.
Park, W. Y., Miranda, B., Lebeche, D., Hashimoto, G. and Cardoso, W. V. (1998). FGF-10 is a chemotactic factor for distal epithelial buds during lung development. *Dev. Biol.* **201**, 125-134.
Partanen, J., Makela, T. P., Eerola, E., Korhonen, J., Hirvonen, H., Claesson-Welsh, L. and Alitalo, K. (1991). FGFR-4, a novel acidic fibroblast growth factor receptor with a distinct expression pattern. *EMBO J.* **10**, 1347-1354.
Petiot, A., Conti, F. J., Grose, R., Revest, J. M., Hodivala-Dilke, K. M. and Dickson, C. (2003). A crucial role for Fgfr2-IIIb signalling in epidermal development and hair follicle patterning. *Development* **130**, 5493-5501.
Poland, A. (1841). Deficiency of the pectoral muscles. *Guys Hosp. Rep.* **6**, 191.
Propper, A. Y. (1978). Wandering epithelial cells in the rabbit embryo milk line. A preliminary scanning electron microscope study. *Dev. Biol.* **67**, 225-231.
Relaix, F., Polimeni, M., Rocancourt, D., Ponzetto, C., Schafer, B. W. and Buckingham, M. (2003). The transcriptional activator PAX3-FKHR rescues the defects of Pax3 mutant mice but induces a myogenic gain-of-function phenotype with ligand-independent activation of Met signaling in vivo. *Genes Dev.* **17**, 2950-2965.
Rice, D. P., Aberg, T., Chan, Y., Tang, Z., Kettunen, P. J., Pakarinen, L., Maxson, R. E. and Thesleff, I. (2000). Integration of FGF and TWIST in calvarial bone and suture development. *Development* **127**, 1845-1855.
Sakakura, T. (1987). Mammary embryogenesis. In *The Mammary Gland: Development, Regulation, and Function* (ed. M. C. Neville and C. W. Daniel), pp. 37-66. New York: Plenum Press.
Schmidt, H. (1998). Supernumerary nipples: prevalence, size, sex and side predilection – a prospective clinical study. *Eur. J. Pediatr.* **157**, 821-823.
Sekine, K., Ohuchi, H., Fujiwara, M., Yamasaki, M., Yoshizawa, T., Sato, T., Yagishita, N., Matsui, D., Koga, Y., Itoh, N. et al. (1999). Fgf10 is essential for limb and lung formation. *Nat. Genet.* **21**, 138-141.
Sengel, P. (1976). *Morphogenesis of Skin*. London: Cambridge University Press.
Stamataki, D., Ulloa, F., Tsoni, S. V., Mynett, A. and Briscoe, J. (2005). A gradient of Gli activity mediates graded Sonic Hedgehog signaling in the neural tube. *Genes Dev.* **19**, 626-641.
Stephens, T. D. (1982). The Wolffian ridge: history of a misconception. *Isis* **73**, 254-259.
Suzuki, K., Yamanishi, K., Mori, O., Kamikawa, M., Andersen, B., Kato, S., Toyoda, T. and Yamada, G. (2000). Defective terminal differentiation and hypoplasia of the epidermis in mice lacking the Fgf10 gene. *FEBS Lett.* **481**, 53-56.
Tao, H., Shimizu, M., Kusumoto, R., Ono, K., Noji, S. and Ohuchi, H. (2005). A dual role of FGF10 in proliferation and coordinated migration of epithelial leading edge cells during mouse eyelid development. *Development* **132**, 3217-3230.
te Welscher, P., Fernandez-Teran, M., Ros, M. A. and Zeller, R. (2002). Mutual genetic antagonism involving GLI3 and dHAND prepatterns the vertebrate limb bud mesenchyme prior to SHH signaling. *Genes Dev.* **16**, 421-426.
Turner, C. W. and Gomez, E. T. (1933). The normal development of the mammary gland of the male and female albino mouse. I. Intrauterine. *Mo. Agric. Exp. Stn. Res. Bull.* **182**, 3-20.
van Genderen, C., Okamura, R. M., Farinas, I., Quo, R. G., Parslow, T. G., Bruhn, L. and Grosschedl, R. (1994). Development of several organs that require inductive epithelial-mesenchymal interactions is impaired in LEF-1-deficient mice. *Genes Dev.* **8**, 2691-2703.
Veltmaat, J. M., Mailleux, A. A., Thiery, J. P. and Bellusci, S. (2003). Mouse embryonic mammogenesis as a model for the molecular regulation of pattern formation. *Differentiation* **71**, 1-17.
Veltmaat, J. M., Van Veelen, W., Thiery, J. P. and Bellusci, S. (2004). Identification of the mammary line in mouse by Wnt10b expression. *Dev. Dyn.* **229**, 349-356.